Scientific Journal of Silesian University of Technology. Series Transport
Zeszyty Naukowe Politechniki Śląskiej. Seria Transport

Volume 116 **2022**

p-ISSN: 0209-3324

e-ISSN: 2450-1549

DOI: https://doi.org/10.20858/sjsutst.2022.116.9

Journal homepage: http://sjsutst.polsl.pl

Article citation information:
Matyja, T., Kubik, A., Stanik, Z. The MEMS-based barometric altimeter inaccuracy and drift phenomenon. *Scientific Journal of Silesian University of Technology. Series Transport*. 2022, **116**, 141-162. ISSN: 0209-3324. DOI: https://doi.org/10.20858/sjsutst.2022.116.9.

Tomasz MATYJA[1], Andrzej KUBIK[2], Zbigniew STANIK[3]

THE MEMS-BASED BAROMETRIC ALTIMETER INACCURACY AND DRIFT PHENOMENON

Summary. MEMS technology has made sensors for measuring barometric pressure and altitude above sea level very cheap and widely used in many consumer electronic devices. This paper presents a theoretical analysis of the sources and types of errors in the barometric altimeter using the standard atmosphere model (ISA). Methods for correcting principal errors caused by non-standard sea level conditions are described and compared. A method of correcting errors in the case of altimeter horizontal movement to the air column and total pressure measurement was proposed. It was compared with another method known from the literature. In the numerical experiment, data recorded by a bicycle computer equipped with a MEMS-based barometric altimeter was analyzed. As the GPS data of the route covered was also known, it was possible to compare the recorded altimeter data with the heights determined from the digital terrain model (DTM), which in this case were considered accurate. The error of the measured altitude calculated in this way was tried to be divided into the principal error, the external error caused by the sensor movement, and the barometer drift. Hence, a numerical experiment was carried out in which, based on the recorded data, an attempt was made to reconstruct non-standard sea level conditions and the impact of speed on the sensor

[1] Faculty of Transport and Aviation Engineering, The Silesian University of Technology, Krasińskiego 8 Street, 40-019 Katowice, Poland. Email: tomasz.matyja@polsl.pl. ORCID: 0000-0001-6364-619X
[2] Faculty of Transport and Aviation Engineering, The Silesian University of Technology, Krasińskiego 8 Street, 40-019 Katowice, Poland. Email: andrzej.kubik@polsl.pl. ORCID: 0000-0002-9765-6078
[3] Faculty of Transport and Aviation Engineering, The Silesian University of Technology, Krasińskiego 8 Street, 40-019 Katowice, Poland. Email: zbigniew.stanik@polsl.pl. ORCID: 0000-0003-1965-4090

measurements. Furthermore, a method of solving such a reverse problem was proposed. The results of the presented studies can be used in the design of systems correcting the indications of barometric altimeters. The accuracy of the altitude measurement is especially important for small controlled flying objects (UAH) and when recording the route of vehicles moving on the ground.

Keywords: barometric altimeter, MEMS, error correction, drift phenomenon, bicycle computer

1. INTRODUCTION

In common opinion, a barometric altimeter is a device used in aviation and parachute jumping, as well as in mountain climbing. However, the uses of the barometric altimeter extend well beyond these areas. This is due to the availability and low price of atmospheric pressure sensors made in the MEMS technology. Today, increasingly, electronic devices are equipped with a barometric altimeter module, which usually works with the GPS system. Thanks to this, it is possible to simultaneously record not only the GPS coordinates of the route but also its vertical profile. Altimeter systems can be found, among others, in smartphones, watches and sports bands, as well as in bicycle computers and devices for tracking and recording the movement of motor vehicles. It is commonly used in drone traffic control and control systems and aviation modeling.

The accuracy of altitude measurements with a barometric altimeter is very important in aviation. This also applies to flights performed by drones (generally UAH). Indeed, instruments used in aviation are usually several classes more accurate than those used, for example, to record routes. For overland travel, the accuracy of the route altitude measurement has no effect on safety but may be significant if the purpose of the tests is to assess the energy needed to travel the route.

This paper discusses the sources and types of errors that occur during altitude measurements with the use of a barometric altimeter. In general, altimeter errors are classified into a fundamental error caused by non-standard sea level conditions: error caused by external conditions, for example, the movement of the pressure sensor to air, and the error resulting from the barometer drift. The authors proposed formulas to estimate the fundamental and external errors. As part of the numerical experiment, data on the altitudes of the route recorded by a bicycle computer were analyzed. These data were compared with the altitudes of the route obtained based on the numerical terrain model, which was considered a reference, and at the same time, accurate. The calculations and simulations were performed in the Matlab environment.

The use of the route recorder on the land was beneficial as it allowed obtaining information about the real altitude; however, on the other hand, it was associated with additional factors that disturb and distort the measurement. It should be noted that a serious problem when measuring pressure while moving near the ground surface is the significant changes in temperature caused by variable insolation and thermal radiation. Various elements of road infrastructure and nearby buildings heat up strongly and disturb the temperature distribution. The temperature of the asphalt is usually higher than the perceived air temperature, which is forecast in the shade and at a height of 2 m from the ground level. The pressure sensor on the cycle computer is approximately halfway up.

2. BAROMETRIC ALTIMETER ERRORS

The barometric altimeter converts the information about pressure into information about the geopotential altitude above sea level based on the well-known formula [1, 3] (Appendix - markings and formulas (A1) - (A5)):

$$h = h_0 + \frac{T_0}{\lambda_0}\left[\left(\frac{p}{p_0}\right)^{-\frac{R\lambda_0}{g_0}} - 1\right] \tag{1}$$

In formula (1), h is the geopotential height, which differs from the real (geometric) height according to the relationship:

$$z = \frac{r_0 h}{r_0 - h} \tag{2}$$

where: r_0 – average radius of the Earth. This difference grows with height, for low altitudes, it is not significant, and at an altitude of 11 km above sea level, it is about 19 m.

The basic element of the barometric altimeter in MEMS technology is a closed aneroid capsule with air under standard pressure. The flexible membrane of the capsule deforms under the influence of external pressure. The capsule material has a defined internal damping and the rate of deformation is not in phase with the deformation itself. The operating temperature of the sensor is also of great importance. Due to this mechanical element, each pressure sensor has a certain inertia and a response delay. Hence, barometers made in MEMS technology can operate on different physical principles for measuring deformation. Piezoresistive strain gauge sensor measures changes in the electrical resistance of resistors mounted on a diaphragm. Capacitive pressure sensor measures changes in electrical capacitance caused by the movement of a diaphragm. In piezoelectric sensors, special materials, that is, quartz crystals or ceramics, generate a charge when pressure is applied [5].

An example of a typical digital barometric pressure transmitter is the Bosch BMP180 sensor based on piezo-resistive technology. The manufacturer states that his device can operate in the pressure range from 300 to 1100 hPa with a maximum pressure resolution of 0.01 hPa. The noise in the high-resolution mode is not less than 0.02 hPa. Figure 1 shows the resolution of the altitude measurement as a function of the pressure measurement resolution, assuming standard atmosphere conditions. It is visible at altitudes of up to 2,000 m above sea level, and the resolution is from 17 to 20 cm. Presently, it is difficult to find a mass-produced sensor with higher resolution in the market.

The measurement error of the barometric altimeter is its characteristic and is inevitable. A well-known phenomenon is the altimeter drift, which is manifested, inter alia, by a continuous and slow change of indications under constant pressure and temperature conditions [14]. Hence, in the literature, there are various attempts to describe this error and various methods of correcting it. Usually, a barometric altimeter is combined with a GPS system. Altitude measurement with the use of GPS is burdened with a significant error and the obtained data without additional information are of little use. After the connection, both systems complement each other, and the appropriate algorithm, based on the Kalman filter [7, 10] or other methods [13], generates the most probable altitude. Another proposed method is to correct

the altimeter indications with the data from the accelerometer and the gyro sensors in combination with the GPS data [8].

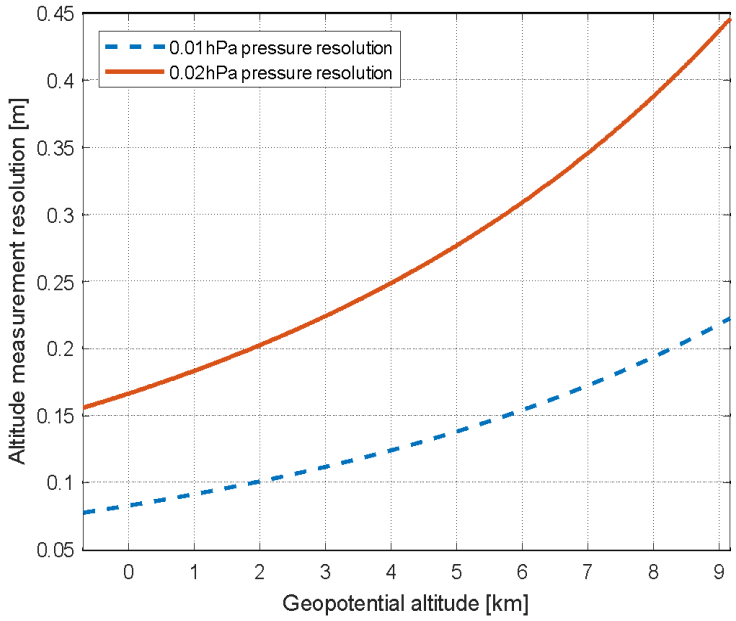

Fig. 1. Altitude resolution corresponding to 0.01 hPa and 0.02 hPa pressure resolution

The authors [9] proposed a stochastic approach to the altimeter error modeling, distinguishing long and short-term errors. In [14], the error of the geopotential height determined by the barometric altimeter was divided into three components:

$$\delta h = \delta h_p + \delta h_e + \delta h_d \tag{3}$$

where: δh_p – principal error, δh_e – external disturbance error, δh_d – drift error.

The principal error δh_p results from the fact that at sea level there are non-standard pressure and temperature conditions $p_0' = p_0 + \Delta p$, $T_0' = T_0 + \Delta T$, and the altimeter has been factory-calibrated to standard conditions. The fundamental error can be estimated from the formula (Appendix - formulas (A6) - (A8)):

$$\delta h_p \approx \frac{RT_0}{g_0}\frac{\Delta p}{p_0}\left(1 + \frac{\Delta T}{T_0}\right) + \left[\frac{R\lambda_0}{g_0}\frac{\Delta p}{p_0}\left(1 + \frac{\Delta T}{T_0}\right) + \frac{\Delta T}{T_0}\right]h \tag{4}$$

In [14], a similar relationship was obtained by expanding the functions of two variables $h(p_0 + \Delta p, T_0 + \Delta T)$ into the Taylor series with respect to the point (p_0, T_0), which, however, did not include the $\Delta p \Delta T$ factor because the expansion was limited to the first derivatives.

The principal error is a function of the measured height. It can also be expressed in the form of dependence on pressure and temperature increases:

$$\delta h_p \approx A(h)\Delta p + B(h)\Delta T + C(h)\Delta p \Delta T \tag{5}$$

where:

$$A(h) = \frac{R}{g_0 p_0}(T_0 + \lambda_0 h)\ \left[\frac{m}{hPa}\right],\ B(h) = \frac{h}{T_0}\left[\frac{m}{K}\right],\quad C(h) = \frac{R}{g_0 p_0}\left(1 + \lambda_0 \frac{h}{T_0}\right)\left[\frac{m}{hPa \cdot K}\right]$$

The results of the calculation of the basic error coefficients (Figure 2) suggest the possibility of neglecting the influence of the last factor related to the product $\Delta p \Delta T$:

$$\delta h_p \approx A(h)\Delta p + B(h)\Delta T \tag{5a}$$

Diston [3], proposed a formula correcting the altitude that considers only the temperature difference ΔT:

$$\delta h_p = h' - h = -\frac{\Delta T R}{g_0}\, ln\, ln\left(\frac{p}{p_0}\right) \tag{6}$$

Interestingly, this formula is formally valid for all layers of the standard atmosphere (ISA). The derivation of formula (6) consists in comparing the two differential equations of the hydrostatic equilibrium of the standard and non-standard (for example, warmer) atmosphere. The assumption about the equality of pressure differentials in these equations seems problematic. In equation (6), the value of the measured pressure p is needed for the correction. If only the measured height h is available, then in the troposphere, the formula (6) can be converted to the form:

$$\delta h_p = \frac{\Delta T}{\lambda_0}\, ln\, ln\,(1 + \frac{\lambda_0}{T_0} h) \tag{7}$$

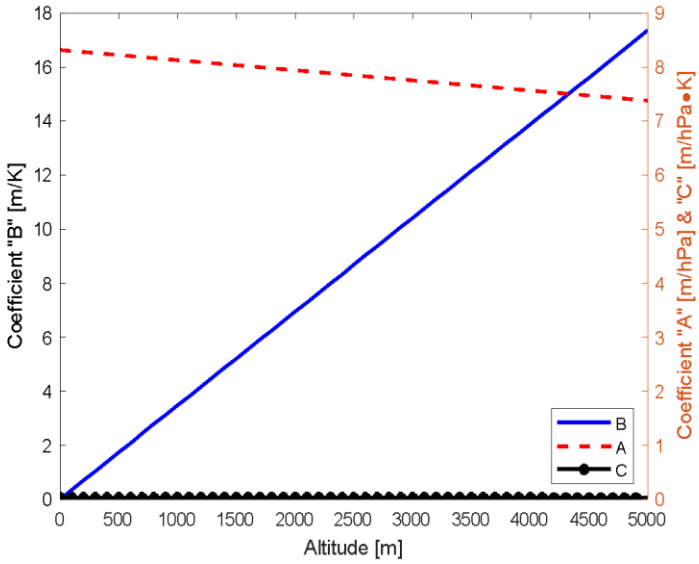

Fig. 2. Values of the gross error coefficients as a function of geopotential height

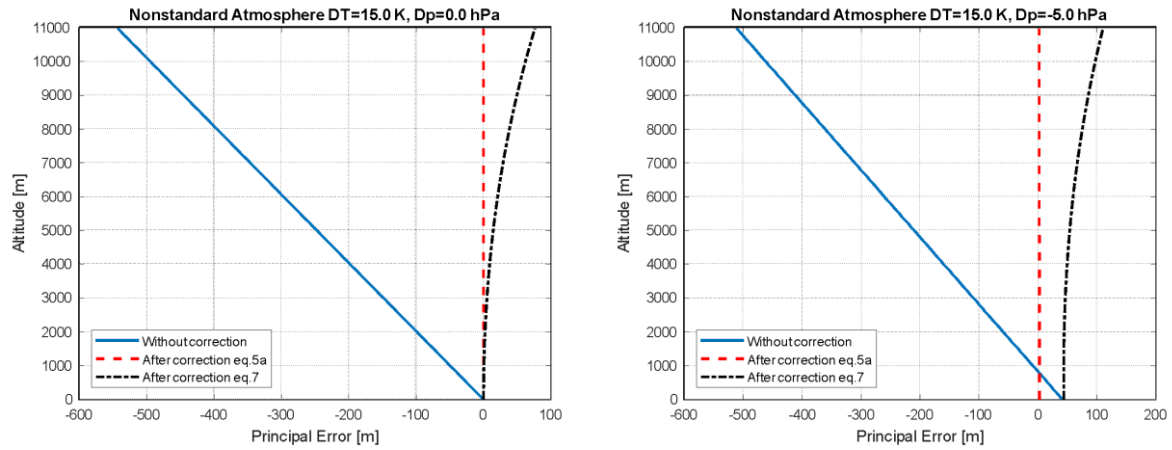

Fig. 3. Principal error in selected non-standard conditions and effects of corrective formulas

It can be assumed that the maximum deviations from the standard temperature are within limits $< -45, +25 >$ °, while the deviations from the standard pressure are within limits $< -50, +50 > hPa$. Using the standard and non-standard atmosphere models $(\Delta T, \Delta p)$, it is possible to determine the altimeter measurement error and the effects of the correction using formulas (5) and (7) in various conditions. Figure 3 shows the results of the basic error correction for the selected two cases of non-standard conditions. As observed, the correction using formula (5a) is effective enough.

Many potential external factors can interfere with pressure sensor measurements (temperature, vibration, air movement, etc.). One of the relatively easily measurable causes of the appearance of external disturbance error δh_e may be the movement of the pressure measurement sensor to air. In [14], this error was estimated by calculating the dynamic pressure based on the velocity of air masses, assuming a constant value of air density under standard conditions (ISA), that is, without considering the changes in density with height. On this basis, a method of correction of altimeter indications has been proposed:

$$\delta h_e = -\frac{T_0}{\lambda_0}\left[\left(\frac{p}{p_0}\right)^{-\frac{R\lambda_0}{g_0}} - \left(\frac{p - \frac{1}{2}\rho_0 V^2}{p_0}\right)^{-\frac{R\lambda_0}{g_0}}\right] \tag{8}$$

where: p – pressure measured, V – wind speed, ρ_0 – air density under standard conditions.

Considering the changes in density with a change in height leads to a slightly different, surprisingly simple, correction formula (derivation in the Appendix - formulas (A9) - (A15)):

$$\delta h_e \approx \frac{V^2}{2g_0} \tag{9}$$

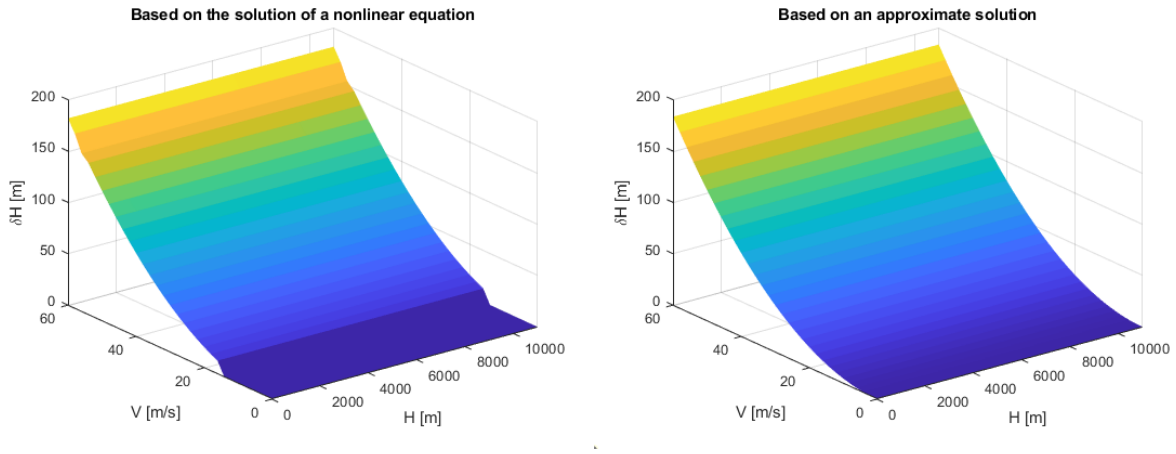

Fig. 4. Numerical solutions and approximate formula for calculations δh_e

The approximation (9) was obtained based on the exact dependence (Appendix - formula (A12)), which can be solved numerically in terms of temperature, and then on its basis, the height error can be calculated. The numerical solution is a function of speed and pressure (altitude). Figure 4 shows the error δh_e calculated numerically and the error calculated from the approximate formula (9). To maintain the relevance of the graphs, the last one is presented in the form of a surface, although in this case, the error is constant given the height. It can be seen that at low speeds, there is a numerical problem in obtaining a non-zero result. At the same time, it can be seen that the approximate solution is accurate enough.

For comparison, Figure 5 shows the error δh_e, which is calculated from formula (8) assuming a constant density and calculated after modifying formula (8) considering the change in density with height. For small heights, formula (8) gives results similar to (9).

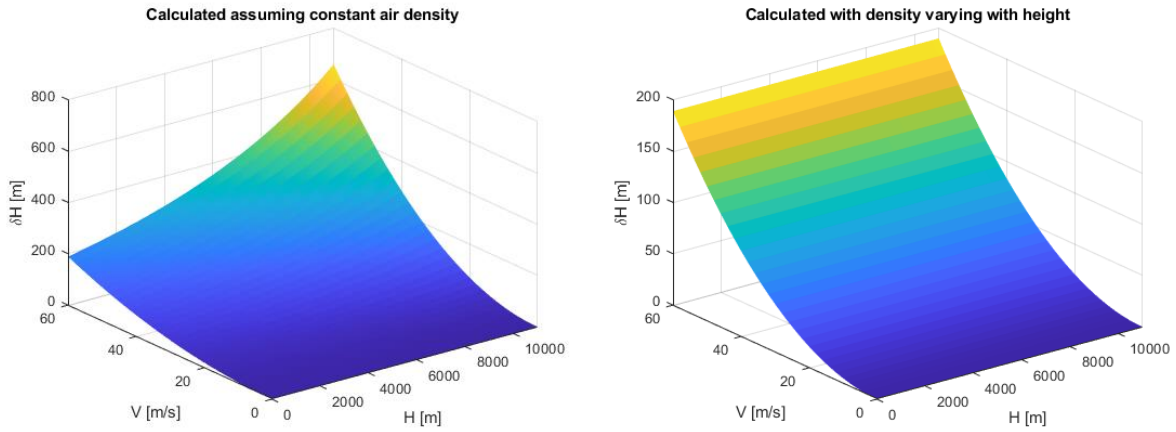

Fig. 5. External disturbance error δh_e calculated from formula (8)

Drift error is hard to describe theoretically. It is a periodically changing signal correlated with slow changes in pressure that may be the result of weather phenomena. Drift also occurs with long-term measurements, and the drift trend may also change over time. The drift signal is non-stationary, but its first derivative shows white noise characteristics. Drift error can be modeled as a stochastic random walk process:

$$\delta\dot{h}_d = w(t) \tag{10}$$

where: $w(t)$ is a white Gaussian stochastic process with zero mean and variance σ^2 deeply dependent on the local weather, season and time [14].

3. NUMERICAL EXPERIMENT

Data recorded by the bicycle computer during the route shown in Figure 6 were analyzed. The journey along the route with a total length of 120 km took just over 5 hours. On that day, the forecast temperature was 29°C, and the pressure was around 1010 hPa, there was a weak wind from the west, the influence of which on the course of the experiment was ignored.

According to the manufacturer of the bicycle computer, the barometric altimeter is initiated when data recording is started and then adjusted with the data from the GPS system. The resolution of data recording with an altitude is 0.2 m, which corresponds to the resolution of typical pressure sensors in the MEMS technology. The recording rate for all data (including GPS coordinates, altitude and temperature) is 1 Hz.

Recorded GPS coordinates were projected onto the map plane in rectangular coordinates using the PUWG 1992 (EPSG2180) reference system [11]. Based on the transformed coordinates of the route, it is possible to determine map sheets on the scale of 1: 5000, which correspond to the digital terrain model (DTM) data sets. These collections are currently available to the public and can be downloaded from the website (https://mapy.geoportal.gov.pl/). According to the information on the website, the height data was obtained through laser scanning (LIDAR) with a resolution of a regular grid of 1 m x 1 m and a declared accuracy of 0.2 m. The data is in text format and requires transformation to matrix form to facilitate computer processing. Files only contain points belonging to the area on the surface of the ellipsoid. Hence, after the projection onto the map plane, the effect of missing information appears on some edges of the rectangular area. As the sheets partially overlap, it is possible to supplement data from adjacent sheets.

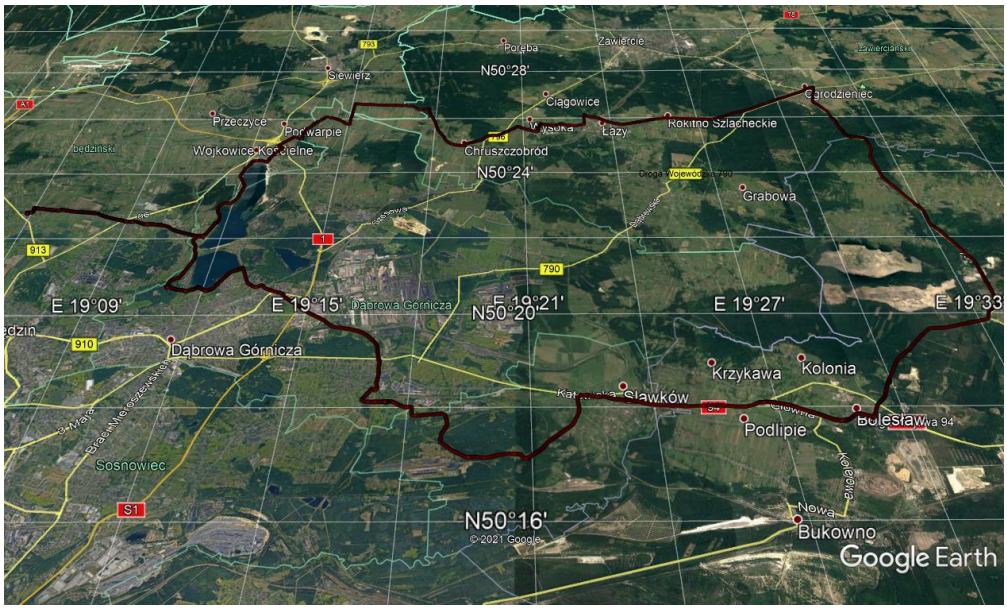

Fig. 6. Recorded route

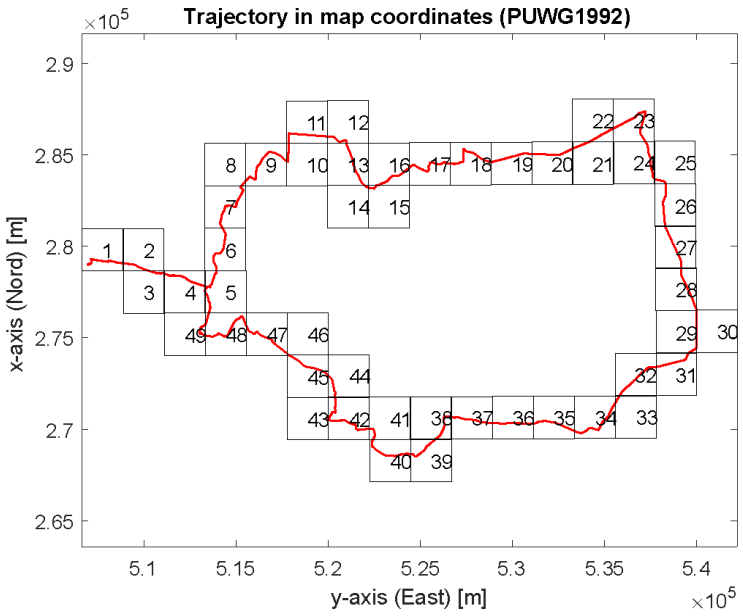

Fig. 7. Determination of height map sheets based on route coordinates

Knowing the trajectory of the bicycle's movement, it is possible to designate the identification number of the required map sheets and the associated DTM data. The automatic procedure for searching for the necessary sheets is illustrated in Figure 7. For example, the first sheet has an identification number: M-34-51-C-c-2-4. Based on the obtained set of the necessary sheets, the appropriate files with the DTM data should be downloaded. It is the minimum set. Due to the above-mentioned feature of the DTM data, there may be a need to download additional adjacent sheets to complete the data at the edges.

The height maps of selected exemplary sheets are shown in Figure 8. Preliminary analysis of the DTM data shows (Figure 9) that in some cases, the data appears to be completely raw, and in others, it appears to be averaged. Perhaps this is because the DTM library was created gradually and at different times, probably with the use of measuring equipment with different technical parameters.

The position of each point on the trajectory in rectangular coordinates can now be referenced to the regular grid DTW, which allows the height to be calculated using Lagrange interpolation. Due to the aforementioned noise of the DTM data, the received height signal is averaged by the median filter of length eight.

Figure 10 shows the route heights recorded by the bicycle computer and obtained from the DTM. As seen, the differences are quite large, although the trend of changes is similar. Treating the data from the DTM as accurate, the "real" error of the altitude measurement by the barometric altimeter installed in the bicycle computer can be determined.

An attempt was made to reconstruct the basic error and the error caused by the movement of the pressure sensor to isolate the drift. The speed at which the bicycle was moving was assumed as the relative speed of the sensor and the air, disregarding the influence of the wind. The speed data recorded by the computer has been dispensed with. Instead, they were determined from the route coordinates by subjecting the obtained signal to smoothing with the median filter (Figure 11). The pressure pickup slots are located on the underside of the cycle computer, where there is positive pressure. As they are closer to the trailing edge, the dynamic pressure will be lower than on the leading edge.

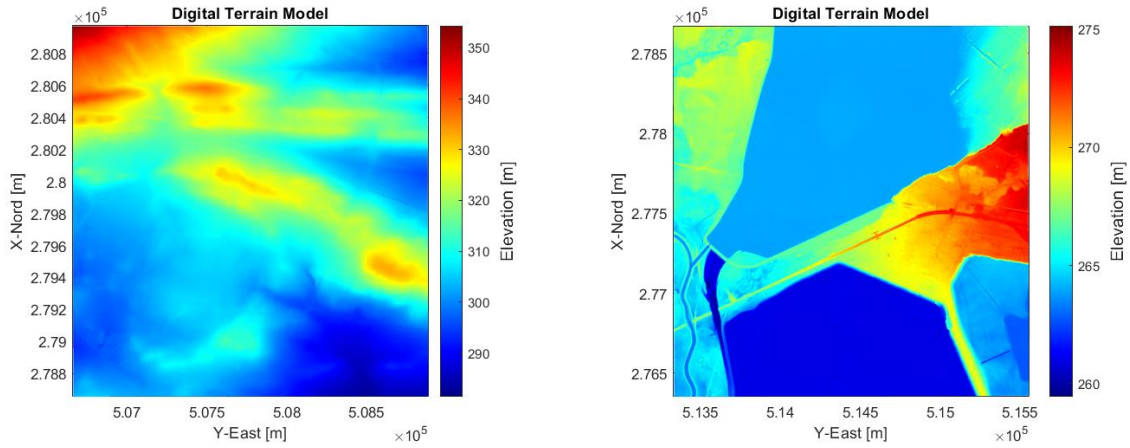

Fig. 8. Sample height maps based on data for sheets 1 and 5

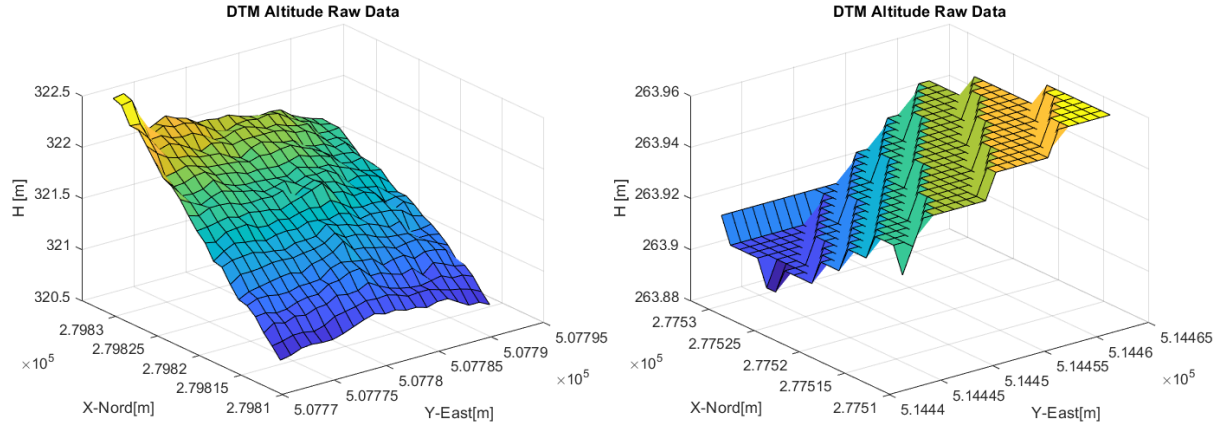

Fig. 9. Smaller fragments of the surface (sheets 1 and 5)

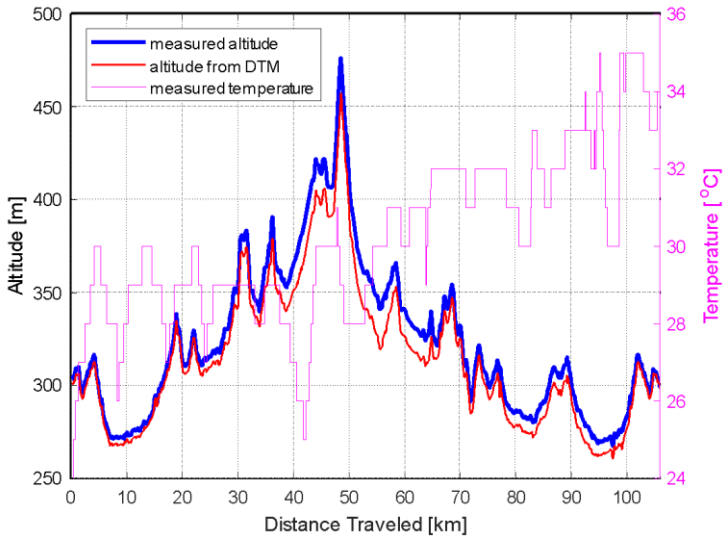

Fig. 10. The altitude of the route recorded and determined from the DTM

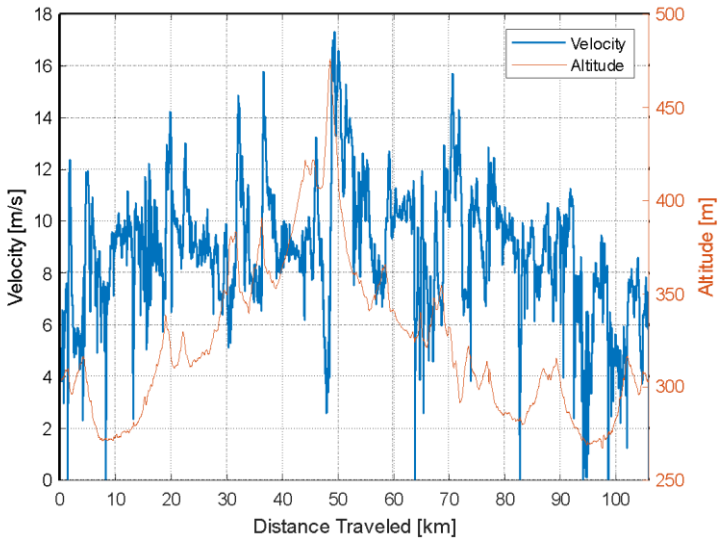

Fig. 11. The speed of the bicycle with a pressure sensor is determined from GPS coordinates

It was assumed that the sum of the measured height h_m and all errors are equal to the actual height h_r from DTM:

$$h_m + \delta h_p + \delta h_e + \delta h_d = h_r \tag{11}$$

The drift will then be equal to:

$$\delta h_d = (h_r - h_m) - (\delta h_p + \delta h_e) \tag{12}$$

The least squares method and the minimization of the functions with constraints were used to reconstruct the non-standard conditions and the impact of speed:

$$f = \frac{1}{2}\sum_{i=1}^{N} (A_i \Delta p + B_i \Delta T + C_i \Delta p \Delta T + D_i \alpha + h_{mi} - h_{ri})^2 \tag{13}$$

where: $A_i = A(h_{mi}), B_i = B(h_{mi}), C_i = C(h_{mi}), D_i = \frac{V_i^2}{2g_0}, N$ – is the number of recorded measurements.

Note that for about a minute, the cycling computer recorded zero altitude, presumably getting a GPS reference altitude during this time. This part of the signal was omitted.

Restrictions have been assumed for the variables $\Delta p, \Delta T, \alpha$, partly due to the weather forecast for the area and the fact that the overpressure may be less than the maximum:

$$\begin{gathered} -5hPa \leq \Delta P \leq 5hPa \\ 15° \leq \Delta T \leq 20° \\ 0 \leq \alpha \leq 1 \end{gathered} \tag{14}$$

The following results were obtained: $\Delta p \approx -2.89 hPa$, $\Delta T \approx 15°$, $\alpha \approx 0$. The last of them proves the negligible influence of driving speed on errors of height measurement. Figure 12 shows the error distribution computed and estimated by the least squares method. After subtracting the errors, a drift signal was obtained (Figure 13), for which the derivative over time was calculated (the results were related to the distance traveled).

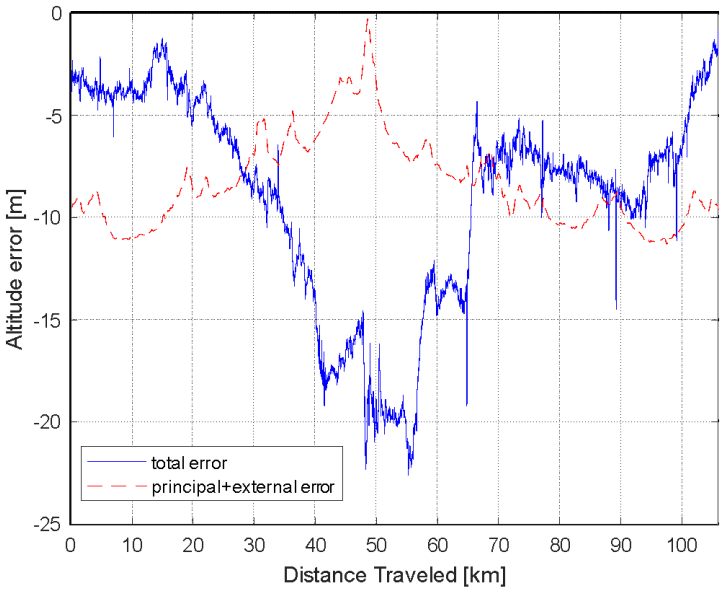

Fig. 12. Total height error and estimated error $\delta h_p + \delta h_e$

The barometer drift obtained with the proposed method is quite large and clearly increases during both uphill and downhill slopes. The derivative signal from drift fulfills in part the characteristic features of white noise. However, there are peaks in it, which may be caused by the altitude adjustment with the GPS signal by the internal algorithm of the cycling computer. However, this cannot be checked, as the bicycle computer is a black box for the user in terms of data processing algorithms.

The effect of correcting the height measured with the estimated error is shown in Figure 14. It is not satisfactory. Probably, due to the long journey time, constant sea level conditions cannot be assumed. This is suggested by the temperature profile measured by the computer during the trip (Figure 10). The thermal radiation of the hot asphalt probably had a great influence on the temperature measurement.

The method proposed above was used for shorter 30-minute sections of height measurement. In this case, the results of the correction turned out to be much better, which means that the increments of $\Delta p, \Delta T$ in formula (13) should not be constant. The modified optimization problem now consists in determining the vector of variables $[p_{0j}, T_{0j}, \alpha]$ minimizing the following function:

$$f = \frac{1}{2}\sum_{i=1}^{N} (A_i \Delta p_i + B_i \Delta T_i + C_i \Delta p_i \Delta T_i + D_i \alpha + h_{mi} - h_{ri})^2 \qquad (15)$$

where: $\Delta p_i = Interp(p_{0j}, N_{Mj}, N, 'pchip')$, $\Delta T_i = Interp(T_{0j}, N_{Mj}, N, 'pchip')$ are the values of the pressure and temperature functions at the measuring points spanning a discrete function of the type $\{T_{0j}, N_{Mj}\}$. The abscissas of the N_{Mj} function are evenly distributed in the range from 1 to N. The number M was determined by dividing the number of measurement points N by 1800 (on average every half an hour). At this stage, it is assumed that the coefficient associated with the external error is constant along the entire route. The constraints (14) were extended to all coefficients $p_{0j}, T_{0j,}$ respectively.

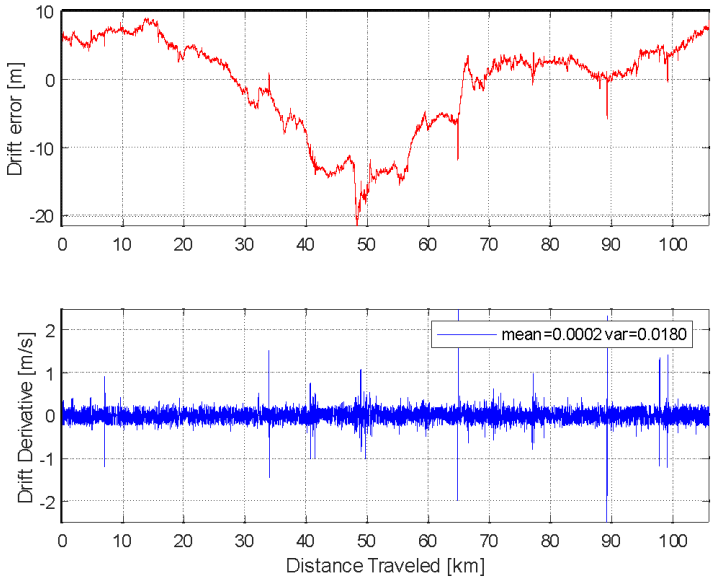

Fig. 13. Barometer drift and time drift derivative

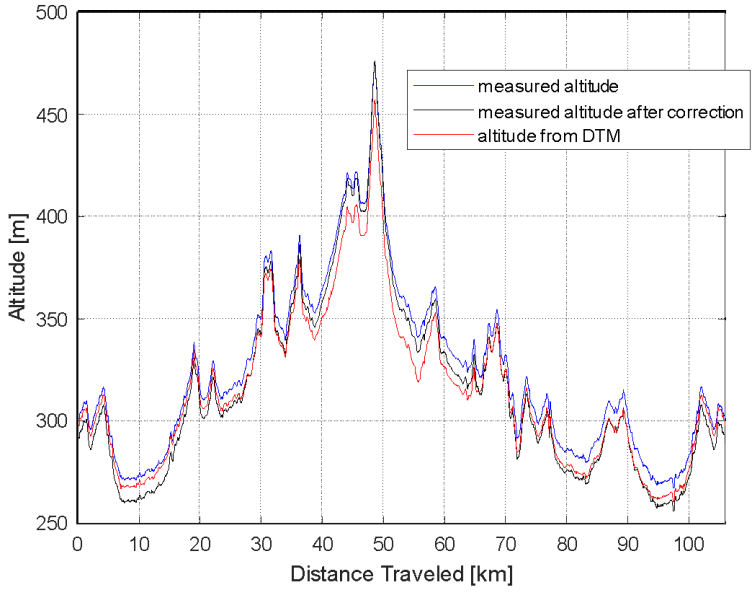

Fig. 14. Effect of correcting the altitude with the estimated error

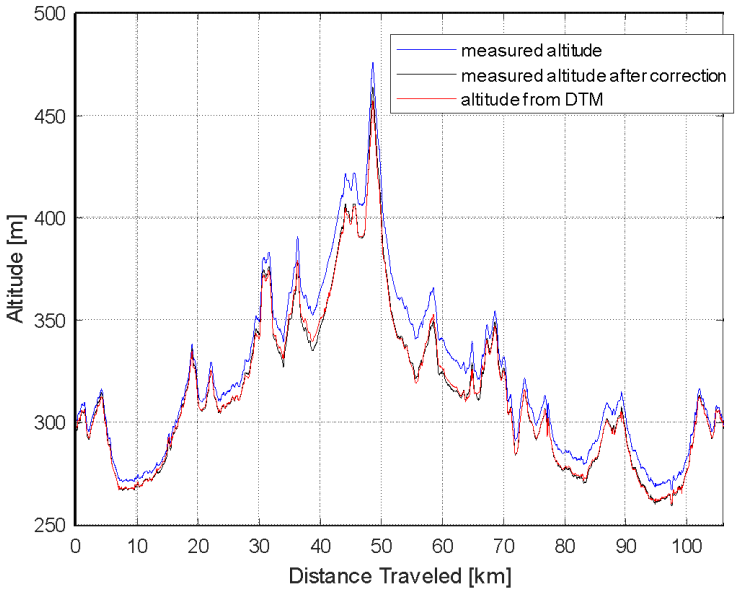

Fig. 15. The effect of correcting the altitude assuming the variability of temperature and pressure over time

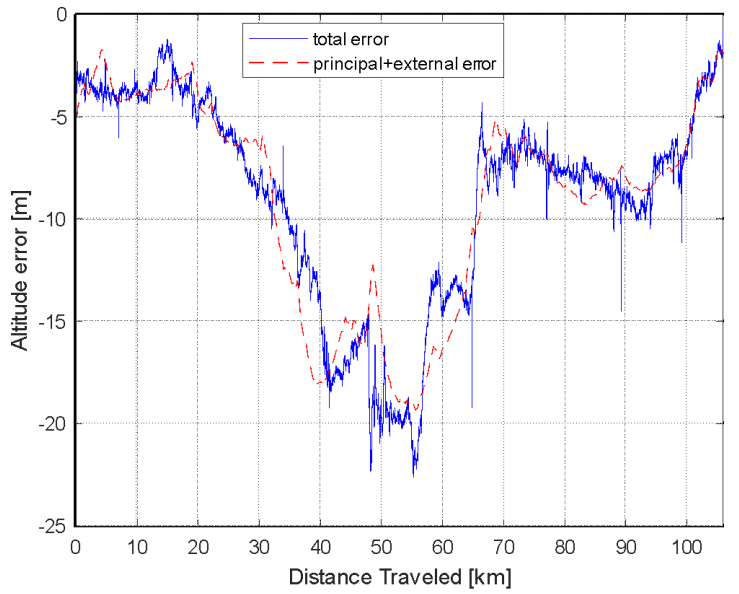

Fig. 16. Comparison of the total error and the error estimated with the assumption of temperature and pressure variability over time

The defined optimization problem (15) requires a bit more computational effort compared to (13). Additionally, in this case, the gradient of the function cannot be easily calculated. Even so, the standard *fmincon* function from the Matlab environment library easily found the local minimum. The effect of correcting the height after the applied changes is shown in Figure 15. It is definitely better than before, which is also visible when comparing height errors (Figures 16). The drift amplitude also decreased (Figure 17). The values of pressure and temperature

correcting the fundamental error, interpolated from the optimization results, are shown in Figure 18. The coefficient of the influence of the sensor speed on the altitude error was $\alpha = 0.0292$.

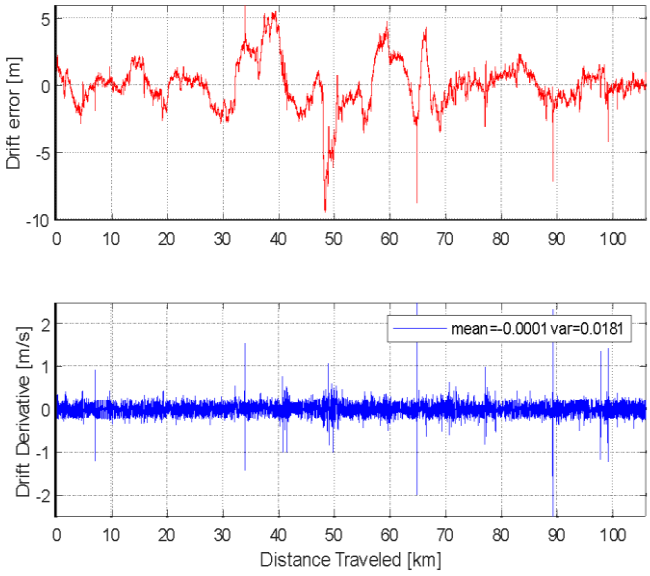

Fig. 17. Drift error (assuming temperature and pressure variability over time)

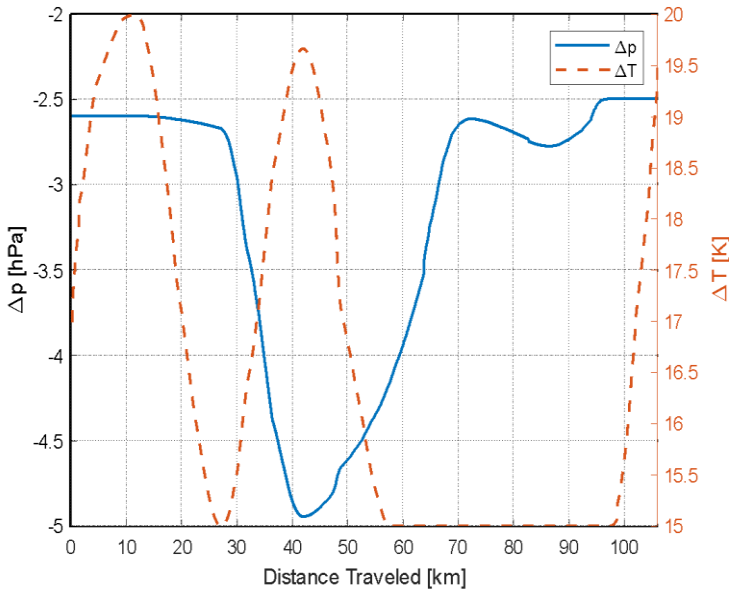

Fig. 18. Changes in pressure and temperature correcting the fundamental error

4. DISCUSSION OF RESULTS

The approximate formula for correcting the fundamental error (4) derived in this paper is basically only a more accurate version of the formula given in the literature [14]. A different derivation technique has been used, which, however, leads to the same goal. Formula (4) differs by an additional non-linear factor, which, as shown by numerical simulations, is much smaller than the linear factors (Figure 2). At the same time, the simulation showed that the height correction using formula (4) is very effective (Figure 3). If for some reason, greater accuracy of the fundamental error correction would be needed, a different, more precise expansion into a series of exponential functions in the exact formula (A7) can be used.

Formula (6) correcting the height only considering the deviation from the standard temperature [3] is shown to be much less effective (Figure 3). Its possible advantage is that it can be used in all layers of the standard atmosphere, practically up to an altitude of 86 km above sea level. In the case of this formula, the authors' assumption about the equality of the differentials of the functions of two different pressure distributions is debatable. By measuring the altitude, and additionally, the temperature at this altitude, it is possible to use formula (6) to iteratively calculate the temperature above sea level (assuming a constant temperature gradient in the troposphere). For correcting the principal error at low heights, formula (6) seems to be of little use.

In the case of an external error caused by the movement of the pressure sensor, the approximate formula (9) presented in the appendix is more accurate than formula (8), in which [14] was assumed constant air density regardless of height. It is also much simpler. The numerical simulations (Figures 4 and 5) also showed that formula (9) is also sufficiently accurate compared to the non-linear relationship (A12) from which it was derived.

The advantage of moving on the ground was the possibility of comparing the registered altitude with the altitude determined based on GPS route coordinates and DTM data. The total error determined in this way turned out to be very large (Figure 10), reaching even 22 m.

However, it was not possible to make a correction using formula (4) because the pressure and temperature conditions related to the sea level were not exactly known. In the case of an external error (9), it was possible to calculate the speed with which the bicycle was moving (the wind speed was omitted, as a weak wind was forecast and the wind speed was not measured). At the same time, it was not known what fraction of the maximum dynamic pressure was measured by the cycling computer.

To separate the drift error from the total error of the altimeter, an optimization method (13) was proposed, which was to recreate the pressure and temperature conditions above sea level and estimate the influence of dynamic pressure on the measurement. The calculation results showed that this method is not very effective if the entire recorded drive is considered (Figures 12 and 14). The method was much better for shorter periods of time. It was concluded that the temperature and pressure increases cannot be treated as constant over time. There is a "conflict of interest" - too short data segments adversely affect the effectiveness of the least squares method, and too long limits the change in pressure and temperature values above sea level. Based on trials, it has been estimated that the acceptable length of the time period is about 30 minutes.

The modified new optimization method (15) allowed to solve this problem using interpolation of additional discrete functions, the values of which were also the searched variables of the minimized function. In this case, it was possible to achieve a significant improvement in the efficiency of correcting the height error (Figures 15 and 16). At the same

time, profiles of changes in pressure and temperature increases during the trip were obtained (Figure 18).

Subtracting the principal and external errors from the total error made it possible to estimate the remaining error - barometer drift. Time derivative analysis of this signal substantially confirmed the hypothesis [14] that drift is a stochastic walk process (Figure 17). Interestingly, the same conclusion applied to the drift error determined by a less accurate method (Figure 13). However, in this case, the average of the derivative signal was twice as large, albeit at the ten-thousandth level. Characteristic peaks are observed in the drift derivative signal, which cannot be present in the white noise signal. They are most likely a result of the cycling computer algorithms that adjust the altitude measured by the barometer using GPS data.

The conducted research should be repeated in the future using a barometric altimeter, or better, a barometer that records only raw data, without any correction. Of course, recreating the conditions above sea level only makes sense if the actual weather data was not available or recorded. This method can never give completely accurate results. The algorithm determines the local minimum in the arbitrarily imposed allowable area, and without a more detailed examination of the minimized function (which is difficult), there is no certainty whether there is a better (optimal) solution.

5. CONCLUSIONS

The theoretical considerations about the sources of errors in the barometric altimeter and the methods of correcting them presented in this paper may be used in practice in the process of designing systems that minimize such errors, supported by additional information, for example, from weather stations, accelerometers and GPS. It is known from the literature that such systems are already in use and that development works are still carried out to improve the effectiveness of altitude measurements. According to the manufacturer's information, the bicycle computer used for the tests has such an altimeter and GPS coupling system.

The numerical experiment performed in this work, which consisted in comparing the measured height with the route height obtained based on DTM data, showed a large measurement error. The proposed method of reconstructing non-standard conditions at sea level and the impact of the sensor movement speed allowed to isolate the barometer drift from the total error signal based on the collected data. In the case of long travel times, it was necessary to consider the variability of conditions at sea level. The determined barometer drift signal satisfies the hypothesis of the stochastic walk process quite well. The observed peaks of the drift derivative signal may indicate the interference of the cycling computer and the altitude adjustment based on GPS data. The method of retrospective reconstruction of sea level conditions alone appears to be moderately effective. It is much better and easier to correct the basic error and the error caused by the sensor movement on a regular basis, which, however, requires access to additional information.

The numerical experiment showed that the speed of movement of the pressure sensor has practically no effect on errors. This may be a sign of the correct positioning of the pressure intake slots on the casing of the cycle computer. The manufacturer claims that he used the results of wind tunnel tests in the design of the computer housing and holder. The evaluation of the proposed formula for correcting the external error still requires independent bench tests in controlled air flow conditions.

Correctly read altitude above sea level is very important during flights. It seems that in the case of the analysis of the travel route on the ground surface, it is of secondary importance.

However, when the aim is to test the energy efficiency of vehicles, this parameter, together with the slope of the route, is of crucial importance.

Appendix

Equation (1) can be derived using three relationships: the equation of static air equilibrium:

$$\frac{dp_s}{dh} = -\rho g_0 \tag{A1}$$

ideal gas equations of state, from which the formula for dry air density follows:

$$\rho = \frac{p_s}{RT} \tag{A2}$$

and assumptions about a constant temperature gradient in the troposphere:

$$\frac{dT}{dh} = \lambda_0 \quad , \qquad T = T_0 + \lambda_0 (h - h_0) \tag{A3}$$

where: p_s - static pressure of the air column, h - geopotential height, ρ - air density, R - the gas constant of dry air, T - air temperature [2], λ_0 - temperature gradient in the troposphere, h_0 - reference altitude (for example, sea level) [12].

Based on equations (A1) - (A3), can be written:

$$\frac{dp_s}{p_s} = -\frac{g_0}{R\lambda_0}\frac{dT}{T} \tag{A4}$$

and after integration within the limits from p_0 to p_s and from T_0 to T, the pressure-temperature dependence is obtained:

$$\left(\frac{p_s}{p_0}\right)^{-\frac{R\lambda_0}{g_0}} = \frac{T}{T_0} \tag{A5}$$

which, after reconsidering (A3), leads to formula (1).

The fundamental error of the altimeter can be estimated as follows. Based on formula (1), and considering the pressure and temperature modifications at sea level $p_0' = p_0 + \Delta p$, $T_0' = T_0 + \Delta T$, the height h'can be calculated corresponding to the new conditions. Without losing the generality of further reasoning, can be assumed that $h_0 = h_0'$ and write:

$$\delta h_p = h' - h = \frac{T_0 + \Delta T}{\lambda_0}\left[\left(\frac{p_0 + \Delta p}{p}\right)^{\frac{R\lambda_0}{g_0}} - 1\right] - h \tag{A6}$$

Convert (A6) to form (A7):

$$\delta h_p = \frac{T_0 + \Delta T}{\lambda_0}\left[\left(\frac{p_0}{p}\right)^{\frac{R\lambda_0}{g_0}}\left(1+\frac{\Delta p}{p_0}\right)^{\frac{R\lambda_0}{g_0}} - 1\right] - h \tag{A7}$$

considering an approximation (A8):

$$\frac{\Delta p}{p_0} \ll 1 \;\rightarrow\; \left(1+\frac{\Delta p}{p_0}\right)^{\frac{R\lambda_0}{g_0}} \approx 1 + \frac{R\lambda_0}{g_0}\frac{\Delta p}{p_0} \tag{A8}$$

and eliminating the measured pressure p from the formula by replacing it with the measured height h, finally leads to formula (4).

If the location of the air inlet to the pressure sensor does not guarantee the measurement of static pressure only, then the sensor does not measure the dynamic pressure resulting from the relative movement of the sensor and the air mass (which may be caused by both the wind blowing and the movement of the sensor in space). It can be assumed that in typical weather conditions, the relative movement of the air and pressure sensor (compound of wind speed and sensor speed) has a direction parallel to the Earth's surface. On the other hand, the static pressure of the air column acts perpendicular to the Earth's surface. The device measures the total pressure, which is the sum of the static and dynamic pressures:

$$p = p_s + \frac{1}{2}\rho V^2 \tag{A9}$$

The formula considers the maximum dynamic pressure at the stagnation point. In fact, the positive pressure at the point of pressure may be less. The air density depends on the static pressure and temperature ($\rho = p_s/(RT)$, hence the measured pressure:

$$p = p_s\left(1+\frac{V^2}{2RT}\right) \tag{A10}$$

At the same time, from the pressure-temperature equation (A5), the formula for the measured (total) pressure can be obtained:

$$\left(\frac{p}{p_0}\frac{1}{1+\frac{V^2}{2RT}}\right)^{-\frac{R\lambda_0}{g_0}} = \frac{T}{T_0} \tag{A11}$$

And after the transformations:

$$\left(\frac{p}{p_0}\right)^{-\frac{R\lambda_0}{g_0}} = \left(1+\frac{V^2}{2RT}\right)^{-\frac{R\lambda_0}{g_0}}\frac{T}{T_0} \tag{A12}$$

Equation (A12) has no analytical solution because of T. It can be solved numerically. Since the factor $V^2/(2RT)$, it is small compared to unity (at speeds of up to 90 m/s – Figure A1), the following approximate formula can be proposed:

$$\left(\frac{p}{p_0}\right)^{-\frac{R\lambda_0}{g_0}} \approx \left(1 - \frac{R\lambda_0}{g_0}\frac{V^2}{2RT}\right)\frac{T}{T_0} = \frac{T}{T_0} - \frac{\lambda_0}{T_0}\frac{V^2}{2g_0} \tag{A13}$$

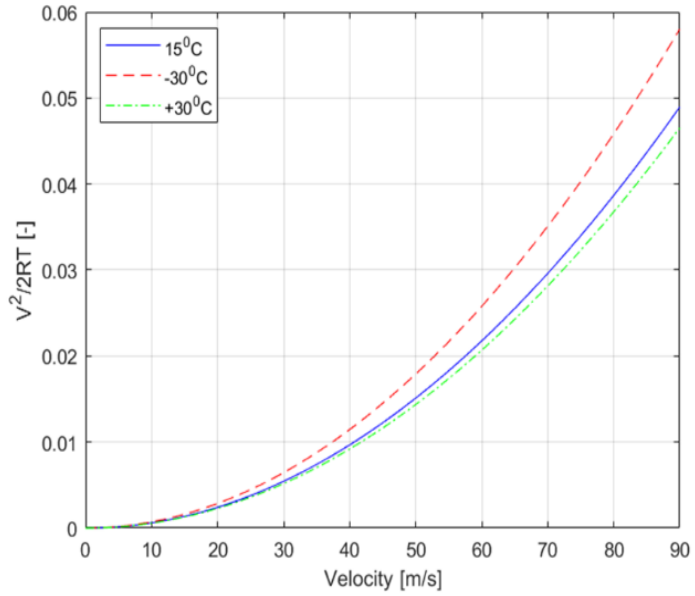

Fig. A1. Dependence of the factor $V^2/2RT$ on speed

After considering the model of the constant temperature gradient in the standard atmosphere and transformations, the formula for height is obtained for the measured pressure and velocity:

$$h \approx h_0 + \frac{V^2}{2g_0} + \frac{T_0}{\lambda_0}\left[\left(\frac{p}{p_0}\right)^{-\frac{R\lambda_0}{g_0}} - 1\right] \tag{A14}$$

Formula (A14) differs from the standard formula (1) in a factor that can be interpreted as the height of the speed. It is also an error resulting from the measurement by the total pressure sensor:

$$\delta h_e \approx \frac{V^2}{2g_0} \tag{A15}$$

References

1. Berberan-Santos M., E.N. Bodunov, L. Pogliani. 1996. „On the barometric formula”. *Am. J. Phys.* 65: 404.

2. Chin E. Lin, Wei-Cheng Huang, Chin-Chung Nien. 2011. „MEMS-Based Air Data Unit with Real Time Correction for UAV Terrain Avoidance". *Journal of Aeronautics, Astronautics and Aviation, Series A* 43(2): 103-110.
3. Diston D.J. 2009. *Computational Modelling and Simulation of Aircraft and the Environment: Platform Kinematics and Synthetic Environment*. Volume 1. John Wiley & Sons, Ltd. ISBN: 978-0-470-01840-8.
4. Dobyne John. 1988. „The Accuracy of Barometric Altimeters with Respect to Geometric Altitude". *Proceedings of the International Technical Meeting of the Satellite Division of The Institute of Navigation (ION GPS 1988).* Colorado Spring, CO, September 1988. P. 451-459.
5. Eswaran P., S. Malarvizhi. 2012. „Design Analysis of MEMS Capacitive Differential Pressure Sensor for Aircraft Altimeter". *International Journal of Applied Physics and Mathematics* 2(1): 14-20.
6. Makoto Tanigawa, Henk Luinge, Linda Schipper, Per Slycke. 2008. „Drift-Free Dynamic Height Sensor using MEMS IMU Aided by MEMS Pressure Sensor". In: *2008 5th Workshop on Positioning, Navigation and Communication. Conference Paper*. 27-27 March 2008. Hannover, Germany. DOI: 10.1109/WPNC.2008.4510374. IEEE Xplore.
7. Nakanishi, H., S. Kanata, T. Sawaragi. 2012. „GPS-INS BARO hybrid navigation system taking into account ground effect for autonomous unmanned helicopter". *IEEE International Symposium on Safety, Security, and Rescue Robotics*: 1-6.
8. Popowski S., W. Dąbrowski. 2008. „An Integrated Measurement of Altitude and Vertical Speed for UAV". Transport and Engineering. Transport. Aviation Transport. *Scientific Proceedings of Riga Technical University*, Series 6, N27. Riga, RTU/2008. ISSN: 1407-8015.
9. Sabatini, Angelo Maria, Vincenzo Genovese. 2013. „A Stochastic Approach to Noise Modeling for Barometric Altimeters". *Sensors* 13(11): 15692-15707. DOI: 10.3390/s131115692.
10. Seo Jaewon, Lee Jang Gyu, Chan, Gook Park. 2004. „Bias suppression of GPS measurement in inertial navigation system vertical channel". *Position Location and Navigation Symposium*: 143-147.
11. Szymanski Zbigniew, Stanislaw Jankowski, Jan Szczyrek. 2012. "Reconstruction of environment model by using radar vector field histograms.". *Photonics Applications in Astronomy, Communications, Industry, and High-Energy Physics Experiments. Proc. of SPIE* 8454: 845422. DOI: 10.1117/12.2001354.
12. U.S. Standard Atmosphere. 1976. U.S. Government Printing Office, Washington, D.C.
13. Whang Ick Ho, Ra Won Sang. 2007. „Barometer error identification filter design using sigma point hypotheses". *International Conference on Control, Automation and Systems*: 1410-1415.
14. Xue Bao, Zhi Xiong, Shouzhao Sheng, Yijie Dai, Sheng Bao, Jianye Liu. 2017. „Barometer Measurement Error Modeling and Correction for UAH Altitude Tracking". *29th Chinese Control and Decision Conference (CCDC)*. IEEE.

Received 11.03.2022; accepted in revised form 04.05.2022